BRAIN CONNECTIVITY
Volume 7, Number 9, 2017

DOI: 10.1089/brain.2016.0483

Integration and Segregation of Default Mode Network Resting-State Functional Connectivity in Transition-Age Males with High-Functioning Autism Spectrum Disorder: A Proof-of-Concept Study

Gagan Joshi,[1–3] Sheeba Arnold Anteraper,[1,3] Kaustubh R. Patil,[1] Meha Semwal,[1] Rachel L. Goldin,[1] Stephannie L. Furtak,[1] Xiaoqian Jenny Chai,[4] Zeynep M. Saygin,[3] John D.E. Gabrieli,[3,5] Joseph Biederman,[1,2] and Susan Whitfield-Gabrieli[3,5]

Abstract

The aim of this study is to assess the resting-state functional connectivity (RsFc) profile of the default mode network (DMN) in transition-age males with autism spectrum disorder (ASD). Resting-state blood oxygen level-dependent functional magnetic resonance imaging data were acquired from adolescent and young adult males with high-functioning ASD ($n = 15$) and from age-, sex-, and intelligence quotient-matched healthy controls (HCs; $n = 16$). The DMN was examined by assessing the positive and negative RsFc correlations of an average of the literature-based conceptualized major DMN nodes (medial prefrontal cortex [mPFC], posterior cingulate cortex, bilateral angular, and inferior temporal gyrus regions). RsFc data analysis was performed using a seed-driven approach. ASD was characterized by an altered pattern of RsFc in the DMN. The ASD group exhibited a weaker pattern of intra- and extra-DMN-positive and -negative RsFc correlations, respectively. In ASD, the strength of intra-DMN coupling was significantly reduced with the mPFC and the bilateral angular gyrus regions. In addition, the polarity of the extra-DMN correlation with the right hemispheric task-positive regions of fusiform gyrus and supramarginal gyrus was reversed from typically negative to positive in the ASD group. A wide variability was observed in the presentation of the RsFc profile of the DMN in both HC and ASD groups that revealed a distinct pattern of subgrouping using pattern recognition analyses. These findings imply that the functional architecture profile of the DMN is altered in ASD with weaker than expected integration and segregation of DMN RsFc. Future studies with larger sample sizes are warranted.

Keywords: autism spectrum disorder; default mode network; resting-state fMRI

Introduction

Autism spectrum disorder (ASD) is a highly morbid neurodevelopmental disorder characterized by varying degrees of deficits in social–emotional functioning along with restricted repetitive behaviors (American Psychiatric Association, 2013) and is estimated to affect up to 2% of children and adolescents in the general population (Blumberg et al., 2013). ASD, in intellectually capable individuals, is characterized by impaired social and emotional awareness, motivation, and reciprocity, cognitive rigidity, and limited perspective taking and introspective ability (Ben Shalom et al., 2006; Blakemore and Choudhury, 2006; Ebisch et al., 2011; Hill et al., 2004; Rieffe et al., 2007; Salmi et al., 2013). The clinical presentation of ASD is highly heterogeneous and the diagnosis of ASD is often delayed, more so in intellectually capable populations where social impairments may not fully manifest until developmentally expected social demands exceed limited capacities (American Psychiatric Association, 2013).

[1]Alan and Lorraine Bressler Clinical and Research Program for Autism Spectrum Disorder, Massachusetts General Hospital, Boston, Massachusetts.
[2]Department of Psychiatry, Harvard Medical School, Boston, Massachusetts.
[3]McGovern Institute for Brain Research, Massachusetts Institute of Technology, Cambridge, Massachusetts.
[4]Departments of Neurology, Johns Hopkins University, Baltimore, Maryland.
[5]Department of Brain and Cognitive Sciences, Massachusetts Institute of Technology, Cambridge, Massachusetts.

While there is strong evidence that autism is associated with abnormal brain development, the nature of the aberrant neural functioning is not well characterized (Muller et al., 2011; Nicolson and Szatmari, 2003). Considering the central role that social deficits play in ASD, neuroimaging research focused on the brain regions associated with social processing is of particular interest. Improved understanding of the neural correlates may help elucidate neural mechanisms and help identify biomarkers that could aid in earlier diagnosis of ASD, before the emergence of clinical markers, and possibly inform pharmacotherapeutic interventions.

Based on the extant literature (Adolphs, 2009; Blakemore, 2008; Di Martino et al., 2009; Frith and Frith, 2007; Mitchell, 2009; Olson et al., 2007), the major brain regions that are typically identified as components of a social processing network include the prefrontal cortex (PFC) regions (medial PFC [mPFC] and orbitofrontal cortex), the limbic regions (regions of medial temporal lobe [amygdalae and anterior hippocampi] and cingulate cortex [anterior and posterior cingulate cortex (ACC and PCC)]), anterior temporal lobes, temporoparietal regions (lateral fusiform gyri [FGs], temporoparietal junction [TPJ]), and anterior insulae (AIs). Emerging neuroimaging literature on functional connectivity (Fc) in autism has identified social task-related hypoactivation of brain regions that subserve the social–emotional brain networks, including the mPFC, ACC, PCC, angular gyrus (AG), right (Rt.) AI, and left (Lt.) FG (Di Martino et al., 2009).

Resting-state (Rs) functional magnetic resonance imaging (fMRI) assesses intrinsic functional brain activity in the absence of an overt task (task independent) (Biswal et al., 1995; Fox et al., 2005; Greicius et al., 2003; Lowe et al., 2000). Brain regions that are simultaneously active during Rs exhibit a positive temporal correlation of associated blood oxygen level-dependent (BOLD) signals, together constituting intrinsic functional networks. Functional networks identified by Rs-fMRI have been shown to be robust and reliable and can thus provide useful information about brain organization differences across different clinical populations and during development (Dosenbach et al., 2010; Seeley et al., 2009). A key advantage of Rs analysis over task-based measures is the absence of possible confounds associated with underlying differences in task performance or in the way the task is executed.

The default mode network (DMN) is one of the most extensively studied resting-state functional connectivity (RsFc) networks. The DMN is an integrated system that supports self-monitoring and social, emotional, interpersonal, and introspective processes (Raichle et al., 2001). It is an endogenously mediated network that is activated at rest and during social/emotional tasks, while it is deactivated by cognitively demanding nonsocial tasks. The DMN is involved in many of the processes that are compromised in individuals with autism, including social and interpersonal cognition (Buckner et al., 2008; Uddin, 2011).

Intrinsic functional brain connectivity is altered in autism with evidence of both hypo- and hyperconnectivity, findings that are possibly reflective of the complex phenotype of the disorder. Although the literature on RsFc of the DMN in ASD suggests both hypo- and hyperconnectivity within the network and reduced internetwork connectivity (Assaf et al., 2010; Barttfeld et al., 2012; Di Martino et al., 2013; Doyle-Thomas et al., 2015; Eilam-Stock et al., 2014; Kennedy and Courchesne, 2008; Lynch et al., 2013; Monk et al., 2009; Mueller et al., 2013; Starck et al., 2013; Uddin et al., 2013; von dem Hagen et al., 2013; Washington et al., 2014; Weng et al., 2010; Wiggins et al., 2011; Ypma et al., 2016; Zhao et al., 2016), the most consistent finding is of reduced RsFc within the DMN with weaker coherence of RsFc between the posterior and anterior subsystems (Assaf et al., 2010; Di Martino et al., 2013; Doyle-Thomas et al., 2015; Eilam-Stock et al., 2014; Kennedy and Courchesne, 2008; Monk et al., 2009; Starck et al., 2013; von dem Hagen et al., 2013; Washington et al., 2014; Weng et al., 2010; Wiggins et al., 2011; Ypma et al., 2016; Zhao et al., 2016).

The internetwork RsFc is derived from varying levels of negative correlations, also known as anticorrelations. While positive correlations serve an integrative role in combining neuronal activity subserving similar function, anticorrelations serve a differentiating role segregating neuronal processes subserving competing functions, a phenomenon typically shared between the task-negative (TN) network, that is, the DMN and brain networks activated during nonsocial task performance (task-positive [TP] networks). Typically, the strength of DMN integration (positive correlation) and segregation (anticorrelation) with the TP network correlates with the level of social–emotional maturity and enhances during early adolescence stage of development (Doyle-Thomas et al., 2015; Sherman et al., 2014; Washington et al., 2014).

RsFc studies in autism have generally focused on examining the positive correlation profile from various seed regions. While study of positive correlations of functional neural activity sheds light on the integrative role of neural functions, it fails to offer information on the concurrent anticorrelated functional brain activity, which offers understanding of the functional segregation between RsFc networks. Between-network connectivity may offer insight into the extent with which these networks interact and share functionally relevant information. For instance, social deficits in autism may be due to a lack of anticorrelation between TN (DMN) and TP networks, leading to failure of suppression and related interference of TP networks during social processing, ultimately resulting in social impairments. However, given that anticorrelations have not been studied in conjunction with positive functional correlations in ASD, this hypothesis remains largely unexplored.

To date, only two RsFc studies in autism have examined anticorrelations in ASD. Kennedy and Courchesne (2008) examined anticorrelations in the context of applying global signal regression (GSR), which introduces artifactual anticorrelations to the results (Anderson et al., 2011a; Kennedy and Courchesne, 2008; Murphy et al., 2009). Anderson et al. (2011a) examined Rs anticorrelations without applying GSR in a wide age range sample of youth and adults with ASD; however, as the seed regions spanned through the entire gray matter (GM), the weaker anticorrelations reported within the ASD group were not specific to the DMN (Anderson et al., 2011b; Murphy et al., 2009). Thus, to the best of our knowledge, no previous study has concurrently examined both positive and negative correlations of intrinsic Fc of the DMN in ASD.

To this end, we characterized the RsFc profile of the DMN in a selected sample of transition-age male individuals with ASD by simultaneously examining RsFc for both positive and negative correlations. We conducted a seed-driven

whole-brain correlation analysis of regions of interest (ROIs) anchored around averages of the literature-based conceptualized major DMN nodes, including mPFC, PCC, and bilateral (Bl.) AG, and inferior temporal gyri (Raichle, 2011). Based on the extant literature, we hypothesized that the profile of the DMN in ASD would reveal a functional dysconnectivity pattern that replicates previous findings of reduced functional integration and, in addition, would document reduced functional segregation of the DMN, in particular with the TP regions (i.e., how the two networks are distinct from each other). Furthermore, we explored the applicability of pattern recognition approaches for acquiring additional insights into the RsFc characteristics and their relationship to the ASD. We used unsupervised machine learning and graph theoretical analyses to study the diversity of the connectivity patterns and identify subtypes of atypical connectivity between the ROIs that may potentially serve as diagnostic neural markers. As an exploratory hypothesis, we examined the between-subject diversity in DMN connectivity that is well documented in populations with ASD.

Materials and Methods

Ascertainment of study participants

ASD participants were recruited from referrals to a specialized ambulatory program for ASD and to a child and adolescent psychiatry ambulatory care clinic at the MGH. The age-, sex-, and intelligence quotient (IQ)-matched healthy controls (HCs) were recruited by advertising for the study. Participants with psychosis, autism, inadequate command of the English language, a full scale IQ <80, or major sensorimotor disabilities (paralysis, deafness, or blindness) were excluded. All participants completed the assessment as detailed below after providing written informed consent following complete description of the study. Human research committees at Massachusetts General Hospital and the Massachusetts Institute of Technology approved this study. To further investigate the reproducibility of our findings, we applied identical analysis on the open-access autism brain imaging data exchange (ABIDE) data set ($n = 59$) contributed by principal investigator Michal Assaf, MD (Olin Neuropsychiatry Research Center [ONRC], Institute of Living, Hartford Hospital and Yale School of Medicine, Department of Psychiatry). Detailed information on the assessment and neuroimaging procedures is provided in the release/website (http://fcon_1000.projects.nitrc.org/indi/abide).

Assessment procedures

Full scale IQ of all study participants (ASD and HC) was assessed with the Vocabulary and Matrix Reasoning subtests of the Wechsler Abbreviated Scale of Intelligence (Wechsler, 1999). The observer-rated Edinburgh Handedness Inventory was administered to assess the Rt. or Lt. laterality of dominance in all the study participants (Oldfield, 1971). Socioeconomic status was measured using the four-factor Hollingshead index (Hollingshead, 1975).

ASD participants. All ASD participants received a neuropsychological assessment, a structured diagnostic interview, and a clinical psychiatric diagnostic interview. The diagnosis of ASD was established by a comprehensive psychiatric evaluation conducted by a board-certified psychiatrist experienced in evaluating ASD (G.J.). The psychiatric diagnostic interview was conducted with the subject and, if available, their parent/guardian(s) and incorporated information from multiple sources when available (e.g., psychiatric records and social services). Based on this clinical evaluation, all ASD subjects met Diagnostic and Statistical Manual of Mental Disorders, Fourth Edition (DSM-IV), diagnostic criteria for autistic disorder, Asperger's disorder, or pervasive developmental disorder not otherwise specified (PDD-NOS).

Youth (<18 years old) with ASD were evaluated by administering the Kiddie Schedule for Affective Disorders and Schizophrenia-Epidemiological Version (K-SADS-E) (Orvaschel, 1994; Orvaschel and Puig-Antich, 1987) to the caretaker (parent/guardian), usually the mother. The K-SADS-E is a semistructured interview that generates current and lifetime Axis-I diagnoses according to DSM-III-R/IV criteria (American Psychiatric Association, 1987, 1994) in children and adolescents. It has been shown to possess acceptable test–retest and inter-rater reliabilities (Chambers et al., 1985). All adults (≥18 years old) with ASD were evaluated by administering the Structured Clinical Interview for DSM-IV (SCID), supplemented with modules from the K-SADS-E to assess childhood diagnoses (First et al., 1996). The SCID was administered to the patients themselves as well as a parent/guardian when available. We combined data from both the direct and indirect structured diagnostic interviews by considering a diagnostic criterion positive if it was endorsed in either interview.

Healthy controls. HCs were screened for ASD traits with the Social Communication Questionnaire (Berument et al., 1999; Rutter et al., 2003).

Neuroimaging procedures

Data acquisition. Neuroimaging data were acquired on a Siemens 3T scanner, MAGNETOM Trio, a Tim System (Siemens AG, Healthcare Sector, Erlangen, Germany), using a commercially available, receive-only, 32-channel, radio frequency brain array head coil (Siemens AG, Healthcare Sector, Erlangen, Germany). Participants underwent a resting fMRI scan for 6 min with the instructions: ''Keep your eyes open and think of nothing in particular.'' Resting scan images were obtained parallel to anterior commissure-posterior commissure (AC-PC), covering the entire brain (interleaved echo planar imaging [EPI] sequence, T2*-weighted images; repetition time = 6 sec, echo time = 30 msec, flip angle = 90°, 67 slices with $2 \times 2 \times 2\,mm^3$ voxels). T1-weighted whole-brain structural images were acquired using the MPRAGE sequence (TR/TE/TI/Flip Angle were 2530 msec/3.39 msec/1100 msec/7°, $256 \times 256 \times 176$ voxels, 1×1.3-mm in-plane resolution, 1.3 mm slice thickness). Online prospective acquisition correction (PACE) was applied to the EPI sequence to mitigate artifacts due to head motion (Thesen et al., 2000). Gradient-adjusted PACE data set was used for further analysis.

ABIDE data set. Resting scan images were obtained on 3T Siemens Skyra (repetition time = 0.475 sec, echo time = 30 msec, flip angle = 60°, $3 \times 3 \times 3\,mm^3$ voxels, Multiband factor of 8). T1-weighted whole-brain structural images were acquired using the MPRAGE sequence (TR/TE/TI/

Flip Angle were 2200 msec/2.88 msec/794 msec/13°, $0.8 \times 0.8 \times 0.8\,mm^3$ voxels).

Creation of seeds of interest. *A priori* seeds of interest for the DMN were independent of our data and were defined as spheres with 5-mm radius centered on previously published foci (Fox et al., 2005; Raichle, 2011) generated using WFU_PickAtlas (Maldjian et al., 2003). Seeds at the network level comprised the average of multiple seeds corresponding to the predefined seed regions (listed in Table 1). The lateral parietal seed was located in the posterior subdivision of the AG bilaterally, which is known to be more strongly functionally correlated with the DMN nodes than the corresponding anterior subdivision (Caspers et al., 2006; Uddin et al., 2010).

Data analysis

Data preprocessing. Rs fMRI data were first preprocessed in SPM8 (Wellcome Department of Imaging Neuroscience, London, United Kingdom; www.fil.ion.ucl.ac.uk/spm), using standard spatial preprocessing steps. Data were slice-time and motion corrected, realigned, coregistered to structural scans, normalized to an MNI template, and spatially smoothed with 6-mm FWHM Gaussian kernel.

Motion artifact detection. ART (www.nitrc.org/projects/artifact_detect) was used to identify outlier data points (TRs) defined as volumes that exceeded three z-normalized standard deviations away from mean global brain activation across the entire volume or a composite movement threshold of 1-mm scan-to-scan frame-wise displacement. There was no significant difference in the total number of outliers between groups. Mean number of outliers in the HC group was 4 and that in the ASD group was 7. In addition, there was no significant difference in the mean head motion parameters between groups ($ASD = 0.11 \pm 0.05$ vs. $HC = 0.098 \pm 0.05$; $p = 0.58$). For the ABIDE data set, a bit more conservative threshold of 0.5 for composite motion was used (scan-to-scan). Although there was no significant difference in the total number of valid scans per group, the maximum head movement in the ASD group was significantly more ($p = 0.05$) compared with the HC group. We have therefore regressed out the effect of maximum motion in the second-level analyses.

Connectivity analysis. RsFc analysis was performed using a seed-driven approach with in-house custom software developed in MATLAB, Conn toolbox (Whitfield-Gabrieli and Nieto-Castanon, 2012; www.nitrc.org/projects/conn/).

Each participant's structural image was segmented into white matter (WM), GM, and cerebral spinal fluid (CSF) using SPM8 (Ashburner and Friston, 2005). To minimize partial volume effects with adjacent GM, the WM and CSF masks were eroded by one voxel and used as noise ROI. Instead of using GSR, the first three principal components of the signals from the eroded WM and CSF noise ROIs were removed with regression (Chai et al., 2012) through an anatomical component-based noise correction approach (aCompCor) (Behzadi et al., 2007). Finally, to minimize the effects of head motion-related confounds, we used the realignment parameters and their first-order derivatives along with the motion outliers as regressors during denoising. A temporal band-pass filter of 0.009–0.08 Hz was applied to the time series.

Table 1. *A priori* Literature-Based[a] Default Mode Network Seeds of Interest

DMN seeds of interest (cluster size = 5 mm³)	*BA*	*MNI (x, y, z)*
Medial prefrontal cortex	32/10	+00 +48 −04
Posterior cingulate cortex/precuneus	31/7	−06 −52 +40
Bilateral posterior angular gyrus	39	±46 −70 +36
Bilateral inferior temporal gyrus	21	+58/−61 −24 −09

[a]Fox et al. (2005) and Raichle (2011).
BA, Brodmann area; MNI, Montreal Neurologic Institute.

Statistical analysis

Seed voxel whole-brain correlation analyses. First-level correlation maps were produced by extracting the residual BOLD time course from the average time course of the *a priori* seed ROIs, followed by computing Pearson's correlation coefficients between that time course and the time course of all other voxels. Correlation coefficients were then converted to normally distributed z-scores using Fisher's transformation to allow for second-level General Linear Model analyses. Second-level between-group *t*-tests were performed for the correlation maps from the ASD and HC groups. An average of the six predefined DMN seeds served as the source ROI. Both positive and negative correlations with the source were investigated. All reported clusters that survived a threshold of $p < 0.005$ (height level) and $p < 0.05$ (corrected for family-wise error at the cluster level) were used as ROIs for further analysis. For the ABIDE data set, group-level independent component analysis (ICA) (Calhoun et al., 2001) was carried out in CONN to explore the DMN independence of seeds to take advantage of the superior temporal sampling (TR = 0.475 sec, 947 time points) of this data set.

Pattern recognition analyses

Machine learning analysis. We used Gaussian mixture modeling (GMM), followed by the Bayesian information criterion (BIC) for model selection (Fraley and Raftery, 2012), to perform unsupervised clustering analysis. We used the mclust package, version 5.0.2, in the R statistical environment 3.2.0 (R Core Team, 2015). GMM fits a given number of Gaussian mixture components to the data. More components increase the number of free parameters, which often leads to a better fit at the expense of model complexity. The tradeoff between the model fit and complexity was controlled using the BIC by penalizing models that are more complex (Fraley and Raftery, 2012). Note that mclust allows fitting models that impose a variety of constraints on the components, such as the orientation and shape of the Gaussians. We tested all 14 models provided in the mclust package. We chose the final model that showed minimum BIC. Fisher's Z-transformed correlations between the mean of the DMN and the regions that survived the second-level Fc analysis were used to describe each subject. In the final matrix with each subject representing a row, the feature vectors

were normalized to have mean of zero and standard deviation of one so that each ROI got equal importance. For visualization purposes, we performed principal component analysis (PCA) (Jolliffe, 2002) and retained the first two components. We used a nine-dimensional space—one dimension per ROI that showed significant difference (for exploratory purposes; height threshold of $p < 0.01$, cluster corrected at $p < 0.05$, false discovery rate [FDR] corrected) between ASD and controls—to represent each subject. To visualize the clustering results, that is, whether the ASD and controls get separated, we performed PCA on these nine-dimensional data and plotted them using the first two dimensions. The standard prcomp function in the R statistical package was used to perform the PCA.

Graph theoretical analysis. For each subject, we calculated the pairwise relationship between the ROIs as the Pearson correlation matrix between the corresponding averaged time series. First, we investigated the average connection strength. The upper triangle of the correlation matrix was Fisher's Z transformed and the absolute values were averaged. This gives a proxy measure for the total inter-ROI connectivity. To gain more insights into the inter-ROI connectivity patterns, we utilized minimum spanning tree (MST) (Tewarie et al., 2015). MST provides a unique and mathematically efficient representation and has been previously utilized with MRI data (Stam, 2014). MST as acyclic graphs provides a concise representation of the relationship between the variables. The data are first represented as a fully connected graph for each subject with one node per ROI, and the edges between the nodes weighted with the Pearson correlation distance (one minus correlation). An MST algorithm then prunes some of the edges such that the graph remains connected while the sum of the distances of the remaining edges is minimized. This provides an interpretable graph topology with, in some sense, only the important connections retained. Finally, the specificity and sensitivity values were reported for the MST-based discrimination between ASD and controls. Specificity was calculated as the proportion of controls (true negatives) who were correctly identified based on MST and sensitivity as the proportion of ASD (true positives) participants who were correctly identified out of the total ASD participants.

Results

Clinical characterization

Participant characterization. All ASD participants ($n = 15$) in this study were native, English-speaking, right-handed (with the exception of one participant) Caucasian males (mean age = 21.6 ± 3.7; range = 16–28 years) with intact intellectual capacity (IQ: mean = 111 ± 10; range = 96–130) (Table 2). HC participants were significantly less frequently Caucasian (50% vs. 93%; $p = 0.02$) and had a significantly higher mean IQ (123 ± 9.2 vs. 111 ± 10; $p = 0.001$) than the ASD participants. For the ABIDE data set, there were 24 ASD participants (20 males, mean age = 21.1 ± 2.9; range = 18–31 years and 4 females, mean age = 24.4 ± 1) and 35 HCs (20 males, mean age = 24.2 ± 3.5; range = 19–30 years and 15 females, mean age = 23.9 ± 2.7). There was no significant difference ($p = 0.46$) in IQ between the two groups (ASD: 114 ± 12.4 (80–146) and HCs: 111.2 ± 10(85–146)).

Phenotypic correlates. Among the ASD participants, 67% (10/15) were diagnosed with autistic disorder, 20% (3/15) Asperger's disorder, and 13% (2/15) PDD-NOS. On the structured diagnostic interview for psychopathology completed at enrollment, seven ASD participants were experiencing attention-deficit/hyperactivity disorder (ADHD) and six were suffering from major depressive disorder (Table 3). The psychotropic treatment status of the 15 ASD

Table 2. Demographics and Clinical Characteristics

	ASD	*HC*	p
Demographics			
Total participants	15	16	
Age (years)			
Mean (range)	21.6 ± 3.7 (16–28)	21.9 ± 3.5 (15–29)	0.82
<18 years	3 (20)	1 (6)	
Gender: male	15 (100)	16 (100)	
Race: Caucasian	14 (93)	8 (50)	0.02
Handedness: right-handed	14 (93)	15 (94)	
Socioeconomic status[a] (class 4 or 5)	1 (6)	U/A	
Full scale IQ (range)	111 ± 10 (96–130)	123 ± 9.2 (105–138)	0.001
Clinical characteristics			
ASD subtypes			
Autistic disorder	10 (67)	N/A	
Asperger's disorder	3 (20)	N/A	
PDD-NOS	2 (13)	N/A	
ASD impairment (lifetime; $n = 14$)			
Mild	0 (0)	N/A	
Moderate	10 (71.4)	N/A	
Severe	04 (28.6)	N/A	

Values expressed as *n* (%) or mean ± standard deviation.
[a]Four-Factor Index of Social Status.
ASD, autism spectrum disorder; HCs, healthy controls; IQ, intelligence quotient; N/A, not applicable; PDD-NOS, pervasive developmental disorder not otherwise specified; U/A, unavailable.

Table 3. Psychiatric Comorbidity with Autism Spectrum Disorder

Psychiatric comorbidity (n = *15)*	*Lifetime*	*Current*
Load of psychiatric comorbidity		
Mean	4 ± 2.48	2.40 ± 2.69
Range	1–10	0–8
≥2	13 (86.7)	7 (47)
Psychiatric disorders		
Attention-deficit/hyperactivity disorder	10 (67)	7 (47)
Any anxiety disorder	11 (73)	7 (47)
Multiple anxiety disorders (≥2)	6 (40)	4 (27)
Major depressive disorder	11 (73)	6 (40)
Bipolar disorder (Mania)	6 (40)	1 (07)
Psychosis	3 (20)	3 (20)

Values expressed as *n* (%) or mean ± standard deviation.

participants at the time of scan was as follows: (1) five ASD participants were medication naïve; (2) five ASD participants were on monotherapy (selective serotonin reuptake inhibitors [SSRIs] = 4; stimulant = 1); and (3) the remaining five participants were on a combination of more than two psychotropic medications. SSRIs (8/10) and stimulants (5/10) were the most common class of psychotropic medications being taken by the ASD participants in this study.

Neural characterization

Within-group ASD and HC Fc maps. At the network level, the Fc maps for the default mode—as derived from the average seed from the six *a priori* DMN nodes—in the HCs were largely similar to what is typically expected. The intrinsic Fc architecture of the DMN in the ASD group was atypical, in particular for (1) the absence of

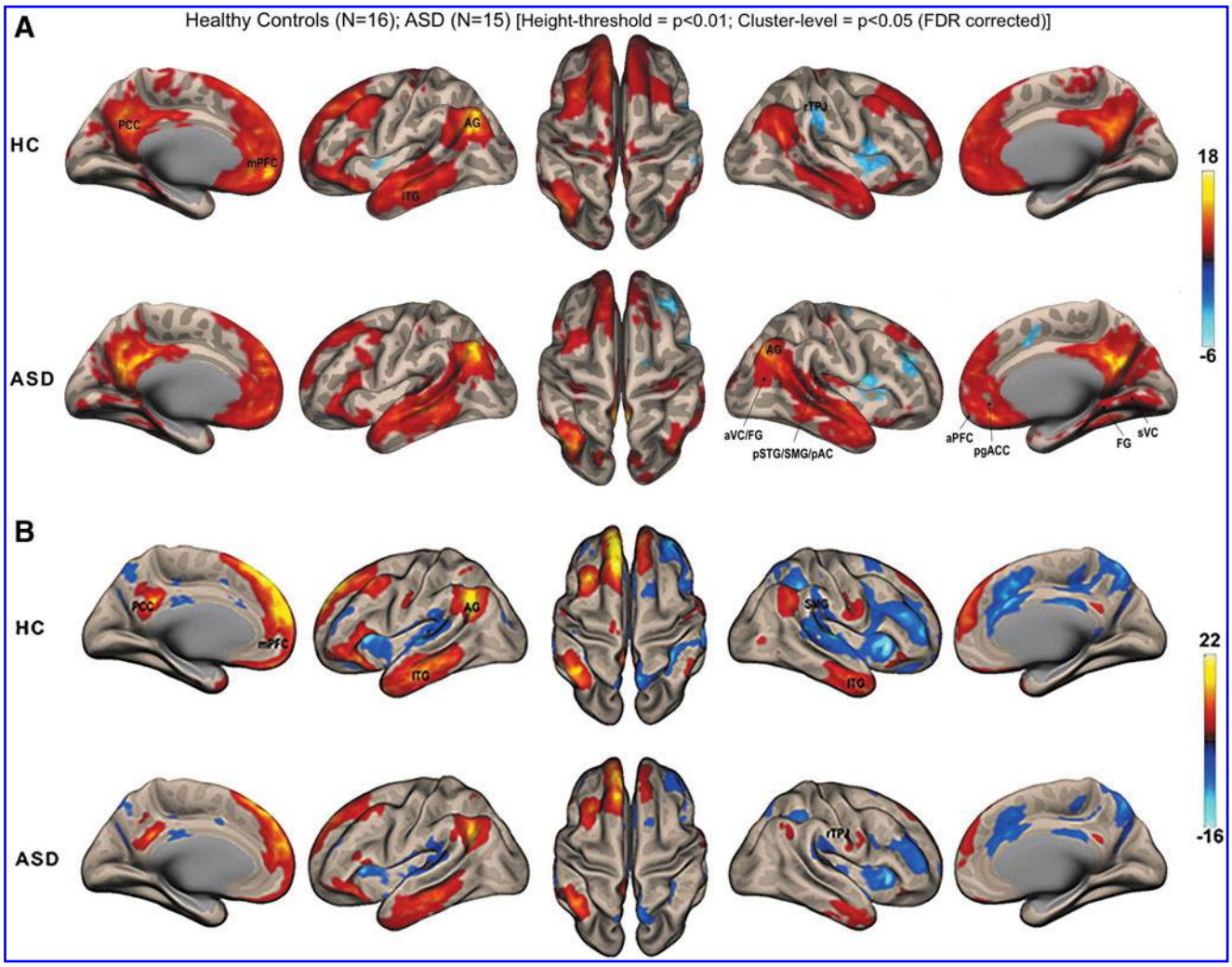

FIG. 1. **(A)** Within-group functional connectivity maps of predefined DMN seed voxel whole-brain correlation analyses. **(B)** Within-group functional connectivity maps of DMN whole-brain group ICA (ABIDE data set). TC: $n = 35$; ASD: $n = 24$. Whole-brain height threshold of $p < 0.001$; two-sided FDR corrected; Cluster-level threshold = $p < 0.05$, FWE corrected. ABIDE, autism brain imaging data exchange; AG, angular gyrus; aPFC, anterior prefrontal cortex; ASD, autism spectrum disorder; aVC, associative visual cortex; DMN, default mode network; FDR, false discovery rate; FGs, fusiform gyri; ICA, independent component analysis; ITG, inferior temporal gyrus; mPFC, medial prefrontal cortex; pAC, primary auditory cortex; PCC, posterior cingulate cortex; SMC, supplementary motor cortex; pgACC, pregenual anterior cingulate cortex; pSTG, posterior superior temporal gyrus; rTPJ, Rt. TPJ; SMG, supramarginal gyrus.

positive correlation with the Lt. cerebellar lobule VIIa region and negative correlations with the Rt. hemispheric TP regions belonging to the lateral FG and associative visual cortex (aVC) and the posterior superior temporal gyrus (pSTG), the supramarginal gyrus (SMG), and primary auditory cortex (pAC); and (2) for the presence of positive correlation with the aforementioned TP regions and with the medial aspect of FG and secondary visual cortical (sVC) region in the Rt. hemisphere (Fig. 1A). Similar atypical Fc architecture of the DMN in ASD was also evident in the ABIDE data set (Fig. 1B).

Between-group ASD and HC Fc network interactions. In the ASD group, relative to the HC group, the RsFc of the DMN seed exhibited (1) significantly lower positive correlations with the Bl. AG regions and mPFC regions of anterior PFC (aPFC) and (2) significantly higher positive correlation with the Rt. hemispheric regions that include the lateral aVC/FG and the pSTG/SMG/pAC Fig. 2A). Results are summarized in Table 4.

For the ABIDE data set, distinctly lower or lack of anticorrelations in Rt. SMG and Rt. pSTG was apparent in the between-group comparison within the ASD group (Fig. 2B). In addition, the correlation analysis between the clinical severity of autism on total autism diagnostic observation schedule (ADOS) and RsFc of the whole brain (DMN component from group ICA) revealed significant positive correlations with DMN Fc with the right hemispheric regions of SMG and pSTG (Fig. 3).

For exploratory analysis of the between-group differences that emerged from our data set using pattern recognition analyses, a height-level threshold of $p < 0.01$ ($p < 0.05$ corrected for FDR at the cluster level) was applied to the second-level

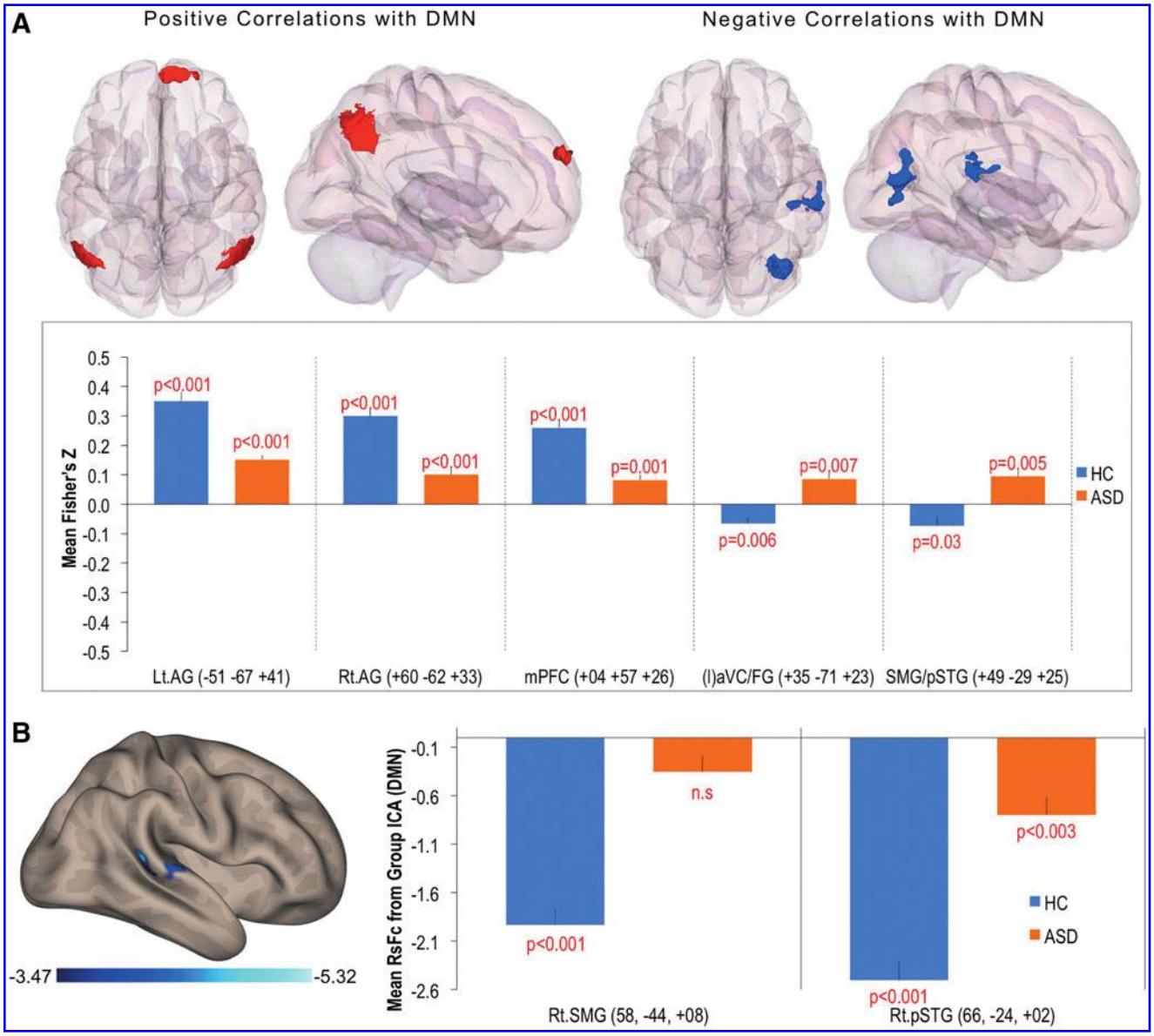

FIG. 2. **(A)** Between-group (HCs vs. ASD) functional connectivity maps of predefined DMN seed voxel whole-brain correlation analyses (whole-brain height threshold of $p < 0.005$). **(B)** Between-group functional connectivity maps of DMN (group ICA) after regressing out the effect of head motion (ABIDE data set, height threshold $= p < 0.001$). HCs, healthy controls.

Table 4. Whole-Brain Seed Voxel Resting-State Functional Connectivity Analysis

DMN combined nodes (mPFC, PCC, BL AG, and BL ITG)	*BA*	*L/R*	*MNI (x, y, z)*	*Cluster size*	*t-Statistic*
ASD ≤ HC					
AG	39	R[a]	+60 − 62 + 33	1678	5.96 ($p < 0.001$)
		L	−51 − 67 + 41	1488	5.68 ($p < 0.001$)
mPFC	10	R	+04 + 57 + 26	1311	4.51
ASD ≥ HC					
SMG/pSTG/pAC	40/22/42	R[a]	+49 − 29 + 25	1296	−4.43
(l)aVC/FG	19/37	R	+35 − 71 + 23	2168	−4.39

Between-group two-sided contrast at $p < 0.005$ voxel-level and $p < 0.05$ cluster-level, FWE corrected.
[a]Regions constitute the right temporoparietal junction.
aAG, anterior angular gyrus; aVC, associative visual cortex; BA, Brodmann area; FGs, fusiform gyri; ITG, inferior temporal gyrus; MNI, Montreal Neurologic Institute; L, left; (l), lateral; mPFC, medial prefrontal cortex; pAC, primary auditory cortex; PCC, posterior cingulate cortex; pSTG, posterior superior temporal gyrus; R, right; SMG, supramarginal gyrus.

between-group DMN seed voxel whole-brain correlation analyses. This allowed us to further investigate the source of the differences in RsFc. There were nine regions that survived the significance test. The three regions that are typically anti-correlated with the DMN in HCs were observed to join the DMN for the ASD group. Box plot representation of ASD versus controls on these nine regions that survived the two-sample *t*-test is shown in Figure 4. Additional ROIs that were identified, in addition to the ROIs identified at the higher threshold of significance, included mPFC regions of aPFC, perigenual ACC, and Lt. cerebellar lobule VIIa (Crus I/II) with significantly lower positive correlations and medial FG/sVC with significantly higher positive correlation.

Pattern recognition analyses. As depicted in the box plot representation in Figure 4, there was marked variability in the individual results of the nine regions that survived the between-group second-level significance tests. These nine ROIs were subjected to clustering analysis.

Clustering analysis. We clustered the pooled 15 ASD subjects and 16 HC subjects using the unsupervised machine learning method as described in the Materials and Methods section. Using the BIC for model selection, we identified five clusters (Fig. 5A). Four of the clusters, two each in the ASD and HC groups, were pure (they contained only ASD or HC subjects), whereas the remaining subcluster had both ASD and HC subjects.

Relationship between ROIs (MST analysis). We probed whether the relationship between the ROIs differs between ASD and HCs. We found that in the HC subjects, the ROIs were significantly more tightly connected than in the ASD subjects (m = 0.37 vs. m = 0.26; *t*-test t(3.35, 19.06), p-value = 0.0033). To gain further insights into the inter-ROI connectivity, we investigated their connection topology using MST (see the Materials and Methods section). We defined two types of ROIs based on their connectivity with the DMN; six positively correlated regions (TN network) and three negatively correlated regions (TP network). Based on the connectivity of those two types of regions within the MST for each subject, an atypical pattern of the TP network regions connecting with the TN network (DMN) regions was observed at a higher rate in the subjects with ASD than HCs (10/15 [67%] vs. 1/16 [6%]; Fig. 5B).

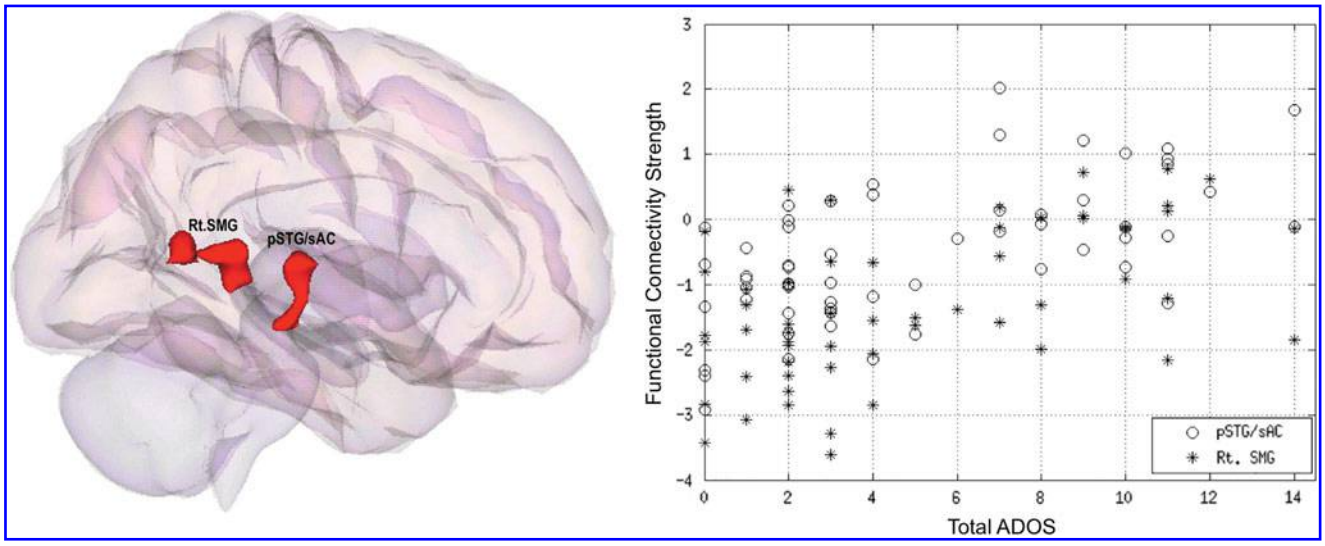

FIG. 3. Whole-brain ADOS revealed positive correlations (r = 0.4) with right supramarginal gyrus (asterisks) and right posterior superior temporal gyrus (circles) after regressing out the effect of maximum head motion from all the subjects at a whole-brain height threshold of $p < 0.005$ ($p < 0.05$, FWE corrected). ADOS, autism diagnostic observation schedule.

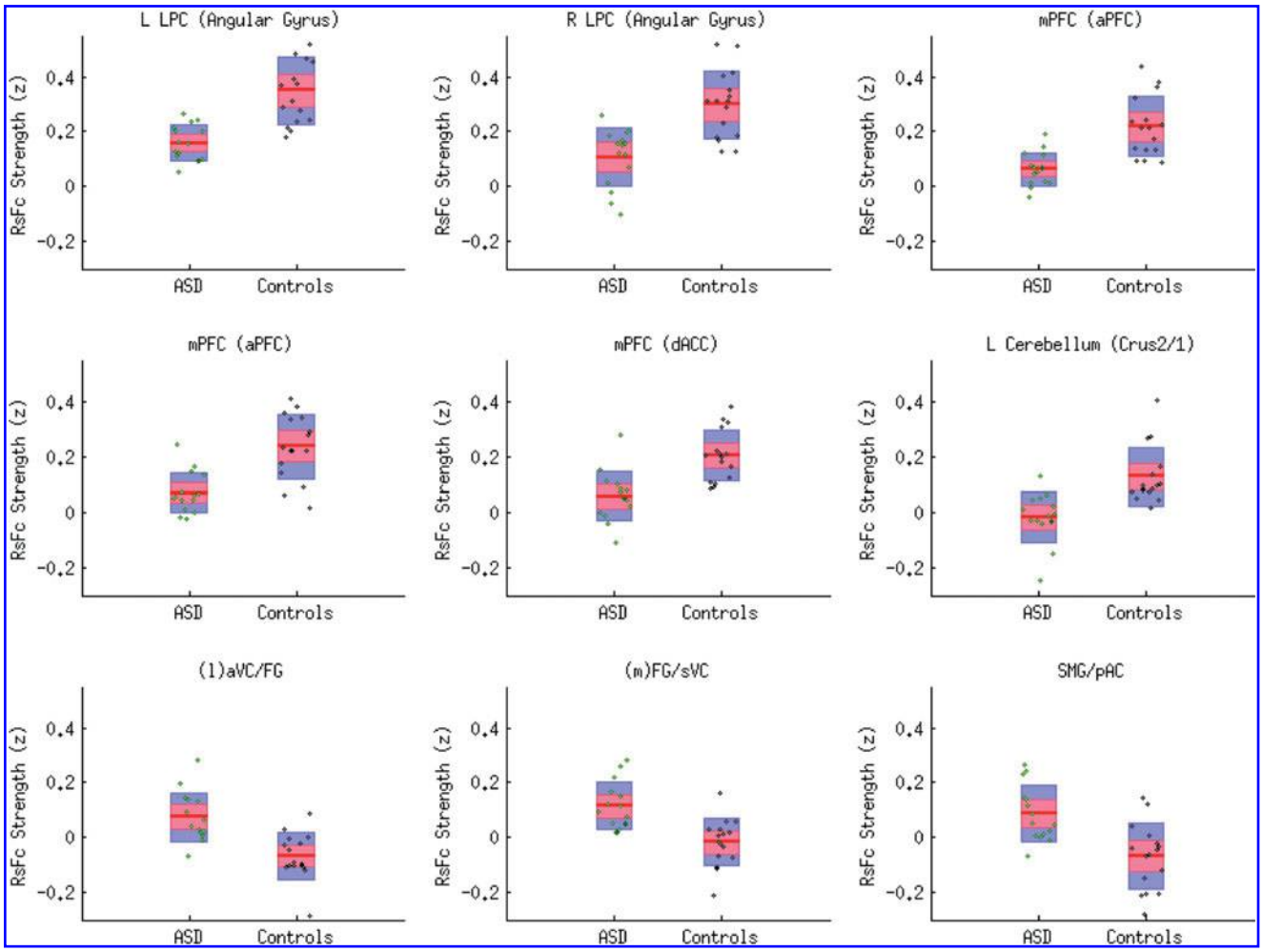

FIG. 4. Box plot representation of ROIs that survived between-group second-level DMN analysis. LPC, left parietal cortex; ROIs, regions of interest; sVC, secondary visual cortical.

Discussion

This study addressed RsFc of the DMN in intellectually capable transition-age males with ASD. Findings in this study suggest that the architecture and strength of the DMN Fc are altered in ASD. The DMN in ASD was poorly integrated with reduced intra-DMN RsFc with the mPFC and Bl. AG regions. In addition, there was significant failure of the DMN to functionally segregate from TP regions in the Rt. hemisphere, which were instead functionally integrated with the DMN, including the regions of FG, visual cortex (VC), AC, SMG, and pSTG. Thus, the Fc architecture of the DMN in ASD was significantly altered with inclusion of the Rt. hemispheric TP regions of FG, VC, SMG, and AC. Notably, there was broad intersubject variability in the strength of the DMN RsFc with brain regions that survived between-group differences. Moreover, based on varying strengths of the DMN RsFc with brain ROIs, the clustering analysis suggests the presence of subgroups with distinct neural profiles, consistent with the typically observed heterogeneous phenotypic expression of ASD. Our findings of weaker functional segregation of the DMN with the TP regions of SMG and pSTG in the Rt. hemisphere were replicated by identical analysis in an independent (ABIDE) data set. To ensure that there is an agreement between the two cohorts, we exported the cluster (Rt. SMG/pSTG) that survived the between-group comparison from the ABIDE sample and used that as a mask for small-volume correction in our data set for ASD>HC comparison. There was a significant overlap of 24 clusters at a cluster-level significance of $p < 0.05$, FWE corrected.

Within-group functional architecture of DMN

The correlation maps for typically developing participants in this study were largely consistent with previous studies in healthy individuals. The functional architecture of DMN in the ASD individuals was atypical for lack of positive RsFc with the Lt. cerebellar region and aberrant positive RsFc with regions in the Rt. hemisphere that are typically anticorrelated with DMN, namely the FG, VC, AC, SMG, and pSTG. Atypical patterns of correlations and significant lack of anticorrelations were evident with the ABIDE data set.

Integration of DMN in ASD (positive correlations)

Our finding of reduced intra-DMN RsFc in ASD is in line with the most consistently reported findings of intra-DMN hypoconnectivity in ASD (Assaf et al., 2010; Barttfeld et al., 2012; Di Martino et al., 2013; Doyle-Thomas et al., 2015; Eilam-Stock et al., 2014; Fishman et al., 2014; Kennedy and Courchesne, 2008; Lai et al., 2010; Monk et al., 2009; Rudie

et al., 2012; Starck et al., 2013; von dem Hagen et al., 2013; Washington et al., 2014; Weng et al., 2010; Wiggins et al., 2011; Ypma et al., 2016; Zhao et al., 2016). Considering the substantial evidence supporting the view that the DMN mediates consideration of one's own thoughts and feelings, or self-referential processing (d'Argembeau et al., 2005; Johnson et al., 2002; Kelley et al., 2002; Moran et al., 2006; Northoff and Bermpohl, 2004; Northoff et al., 2006; Whitfield-Gabrieli et al., 2011), poor functional integration of the DMN may account for diminished capacity for self-referential processing in autism. As the DMN also facilitates a state of readiness to respond to environmental changes, reduced functional integration of DMN may also account for poor awareness and response to surroundings in ASD (Raichle and Gusnard, 2005).

Among the major nodes of DMN, the mPFC and Bl. AG were poorly integrated with the network in ASD. In particular, the aPFC region of mPFC was underconnected with the DMN. The aPFC is proposed to play a major role in the highest level of integration of information received from visual, auditory, and somatic sensory systems to achieve amodal, abstract conceptual interpretation of the environment (Christoff et al., 2003; Petrides and Pandya, 2007). The aPFC may also play a role in influencing abstract information processing and the integration of outcomes of multiple cognitive operations (Ramnani and Owen, 2004). Thus, poor intra-DMN Fc of aPFC may relate to the deficits in abstracting abilities and sensory processing in ASD. Typically, the medial aspect of aPFC is functionally and anatomically connected with the major DMN regions of the mPFC, PCC, and lateral parietal cortex (Liu et al., 2013). Whether the reduced Fc of the DMN with aPFC in the ASD sample of this study can be corroborated with aberrant structural connectivity remains to be investigated.

The AG is a functionally heterogeneous region typically involved in semantic processing bilaterally and, as a component of Rt. TPJ (rTPJ) in conjunction with the SMG, is engaged in attention processing (Decety and Lamm, 2007; Igelstrom et al., 2015; Kubit and Jack, 2013; Scholz et al., 2009). Recent functional neuroimaging literature suggests that impaired functioning of Rt. AG in ASD correlates with severity of inattention and social deficits (Redcay et al., 2013; You et al., 2013). Additionally, reduced RsFc of the Lt. AG in ASD inversely correlates with autism severity (Kennedy and Courchesne, 2008; von dem Hagen et al., 2013). Hence, our finding of reduced integration of Bl. AG with the DMN is consistent with the prevailing literature.

Segregation of DMN in ASD (negative correlations)

In addition to poor integration of the DMN in ASD, there was evidence of poor functional segregation with the TP regions in the Rt. hemisphere. The typically expected correlational directionality of the extra-DMN connectivity with TP regions in the Rt. hemisphere was inversed from negative to positive, suggesting that instead of being suppressed, certain anticorrelated regions are coactivated with DMN in ASD. Positive correlations reflect an integrative role in combining neuronal activity subserving similar functions, whereas anticorrelations signify segregation of neuronal processes that subserve opposite functions or competing representations. Furthermore, the ability to switch between the DMN and TP network relies on the strength of anticorrelations between these two networks that facilitates toggling between competing introspective and extrospective attentional demands (Broyd et al., 2009). Based on this understanding, one could speculate that our findings of the lack of anticorrelations and atypical linkage of TP regions with the DMN may reflect a functional failure of TP network deactivation and aberrant activation, consequently altering the functional relationship between the DMN and TP networks in ASD. This may clinically translate as compromised self-referential processing and impaired ability to switch between introspective and extrospective neural processes.

The RsFc of the DMN with the FG was atypical in ASD. The lateral aspect of Rt. FG exhibited atypical functional integration with the DMN. The nature of DMN RsFc with the lateral FG and aVC brain region, which is typically segregating (Fox et al., 2005), was paradoxically integrating in ASD. The FG has been the subject of previously identified abnormality in brain imaging studies of autism (Corbett et al., 2009; Pierce and Redcay, 2008). Hypoactivation and reduced Fc of the FG to frontal regions have been reported in autism during facial processing tasks (Critchley et al., 2000; Kleinhans et al., 2008; Koshino et al., 2008; Pierce et al., 2001; Schultz et al., 2000). Thus, atypical Fc of the Rt. lateral FG/aVC may relate to poor attention to facial expressions and nonverbal communication deficits observed in ASD.

In this study, the DMN in ASD was atypically correlated with the Rt. hemispheric regions of AG, SMG, and pSTG. Taken together, these regions constitute the rTPJ, which plays a critical role in processing social cognition, empathy, and reorienting attention (Decety and Lamm, 2007; Kubit and Jack, 2013). Abnormal functional activity of TPJ has been documented in individuals with ASD during social task-related activity (Di Martino et al., 2009) or at rest (Anderson et al., 2011b; Fishman et al., 2014; Igelstrom et al., 2016; Lai et al., 2010; Mueller et al., 2013; von dem Hagen et al., 2013). Consistent with our findings, abnormal functional activity of rTPJ and its connectivity are increasingly being implicated in the pathophysiology of ASD (Igelstrom et al., 2016; Mueller et al., 2013; Pantelis et al., 2015; von dem Hagen et al., 2013).

The DMN in ASD, as opposed to in HCs, was positively correlated with the Rt. SMG. As functional components of rTPJ, the SMG is typically recruited for reorienting and maintaining attention on externally oriented nonsocial tasks

FIG. 5. **(A)** Unsupervised clustering of subjects based on the correlation between predefined DMN seed and the nine ROIs that survived between-group second-level DMN analysis. First two principal components applied for visualization purpose; each subject is identified by numbers; each cluster is represented by a different color. **(B)** Minimum spanning tree (MST) of individual subjects from the nine ROIs that survived between-group analysis at the second level. Shades of blue: positively correlated nodes with the DMN; shades of yellow: negatively correlated nodes with the DMN. Red frame: atypical topology; green frame: typical topology (defined as cohesive cluster of positively correlated nodes).

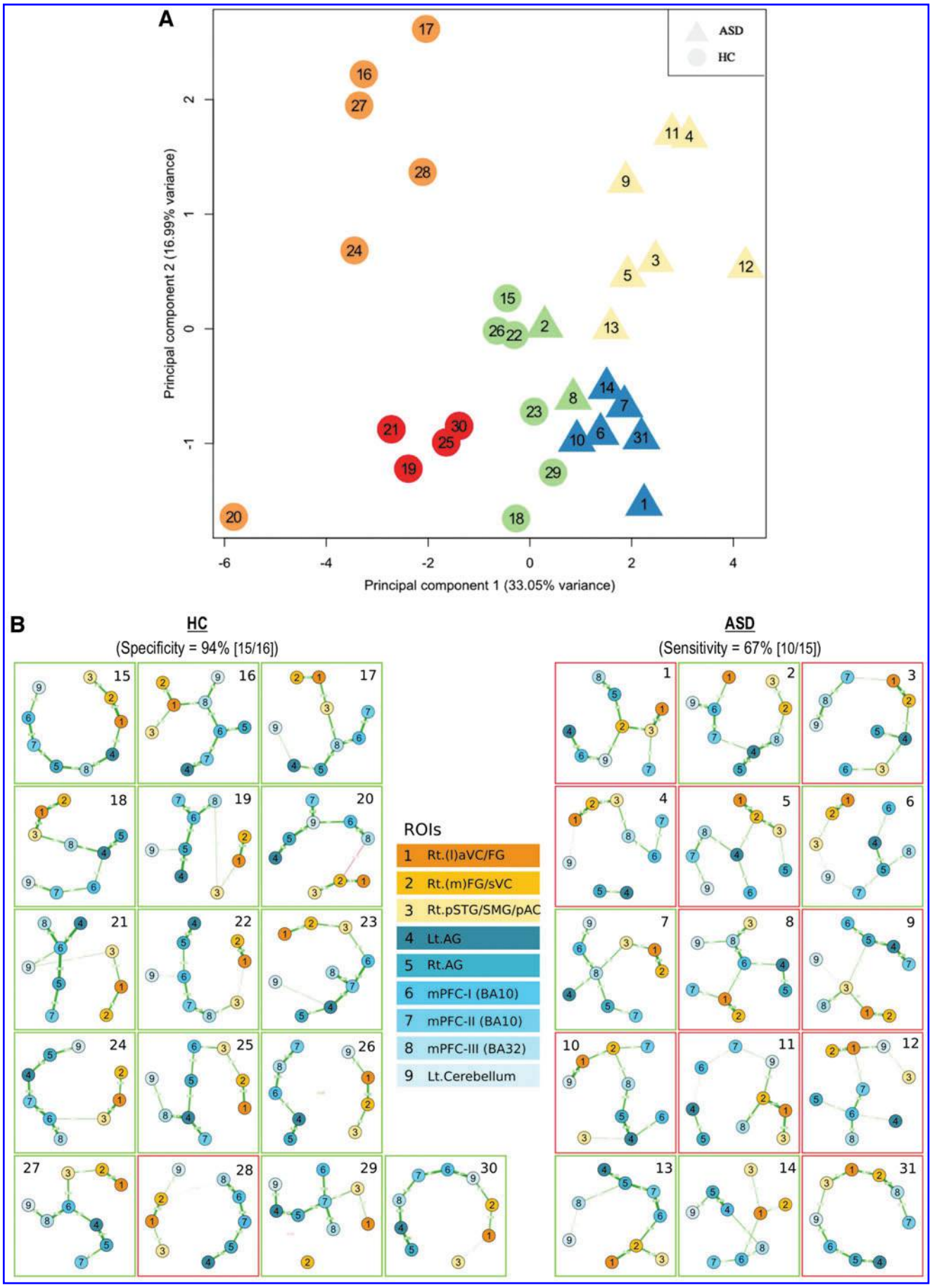

and the AG is functionally engaged in social cognitive processes. Typically, SMG and AG (as part of rTPJ) share anticorrelated patterns of RsFc that reflect the opposing nature of their functional relationship. For example, nonsocial task-based activation of SMG (as part of TP network activation) suppresses AG, which in turn deactivates the DMN. Thus, our results suggesting a lack of anticorrelation between SMG and DMN in ASD may have bearing on the ability of the rTPJ to suppress DMN during TP activity. Additionally, atypical integration of the DMN with SMG in ASD suggests interfering activation of TP regions during introspective and social–emotional activity. Previous studies in ASD have reported SMG impairments in the context of social skill impairments (Abrams et al., 2013; Salmi et al., 2013). Failure to suppress the DMN during TP activation may also present as poor reorienting ability and attentional difficulties that are often associated with ASD. Specifically, activation of SMG during DMN activity may adversely affect social–emotional processing and performance in individuals with ASD.

The ABIDE data set analysis revealed a significant lack of anticorrelation between the DMN and Rt. hemispheric regions of SMG and pSTG. In addition, significant correlation was observed between the strength of anticorrelation between the DMN and Rt. SMG/pSTG and the severity of autism on the ADOS (total score). Specifically, reductions in anticorrelations corresponded positively with symptom severity. This further highlights the importance of examining the anticorrelations in the study of DMN in ASD.

Pattern recognition performance in ASD

Wide variability was observed in the RsFc strength of mean DMN seeds to ROIs that survived between-group second-level DMN analysis, suggesting heterogeneity in the RsFc neural profile in ASD. This heterogeneity was further emphasized in the clustering analysis that noted the presence of subgroups with distinct neural profiles. The neural heterogeneity with ASD observed in this study is consistent with the heterogeneous phenotypic expression of ASD.

Remarkably, all ROIs that survived the second-level between-group DMN analysis belonged to either the TN, that is, DMN (mPFC, Bl. AG, Lt. cerebellar lobule), or TP network (Rt. hemispheric FG, VC, SMG, pSTG, AC). On further assessment of these nine regions that survived the second-level between-group significance tests, we found that interconnectivity between these regions was significantly weaker in the ASD subjects. Thus, the nine identified ROIs not only differed in their connectivity with the DMN but also in their connectivity with each other. Furthermore, by inspecting the MSTs, we could probe differences in the topology of ROI connections between the HC and ASD subjects. We defined two types of ROIs based on their connectivity with the DMN; six positively correlated and three negatively correlated ROIs. The MSTs revealed that in HCs, the two types of ROIs were more tightly connected within their own types, while in ASD, this pattern seems to be disrupted, as observed by the intermixing of the two types of ROIs (Fig. 5B). The atypical MST topology (characterized by anticorrelated TP regions integrated with TN DMN regions) was more frequently present in ASD (67%) than HC (6%) participants. Our results suggest that the topology of connections, in addition to connection strengths, can potentially serve as a marker for identification and quantification of ASD. We speculate that such analysis of topology of connections between brain regions could pave a way for identifying neural markers for the diagnosis of ASD.

Limitations

Our study involved a small sample of intellectually capable Caucasian males with ASD and co-occurring psychiatric conditions. Although nonparametric approaches are ideal for accounting for false positives, we resorted to standard parametric approaches because of our small sample size. Since previous studies have proven the test-retest reproducibility of DMN at 3 Tesla (Meindl et al., 2010) with a small sample size ($n = 18$), we have limited our explorations to DMN. Alterations in the DMN are observed with various neuropsychiatric disorders, including ADHD, mood disorders, and schizophrenia (Castellanos et al., 2008; Drevets et al., 2008; Garrity et al., 2007; Greicius et al., 2007). More detailed studies are needed to identify disorder-specific changes in the DMN. The impact of comorbidity and associated medication treatment might be potential confounds. Although the age range of ASD participants represents transition-age individuals, our findings remain subject to brain developmental-related differences. Employing superior spatial resolution in this study without compromising on whole-brain coverage resulted in a lower temporal resolution and therefore a low number of total time points per subject. Employing simultaneous multislice imaging techniques in future studies would avoid such limitations (as evident from the ABIDE sample) and provide statistical power enhancements (Setsompop et al., 2012) and rigorous execution of denoising strategies. Furthermore, we recognize that the clustering and MST results would be more informative with a larger sample. Nonetheless, our current novel analysis paves the way for new methodologies. We speculate that MST topology, identified using correlations and anticorrelations between ROIs, can reveal additional information about individual differences in ASD; we leave this for future research.

Conclusions

Despite these limitations, results of this study highlight that the RsFc profile of the DMN in transition-age males with HF-ASD was atypically characterized by reduced integration and lack of segregation from regions that typically belong to the TP network. In addition, this study offered proof of concept on the applicability of pattern recognition analysis techniques for identifying subclusters that share distinct profiles of DMN RsFc with brain ROIs and for mapping the individual MST profiles of the inter-ROI RsFc relationship between the DMN and TP network regions identified in this study as atypical in ASD. The preliminary findings of an atypical RsFc profile of the DMN in ASD, as identified in this pilot study, hold the potential to serve as diagnostic neural markers and warrant future investigation in larger samples of the ASD population.

Acknowledgments

This work is funded, in part, by the Alan and Lorraine Bressler Clinical and Research Program for Autism Spectrum Disorder, the Saylor Family Fund for Autism Research,

the MGH Pediatric Psychopharmacology Council Fund, and by the National Institute of Mental Health grant awarded to Gagan Joshi (#K23MH100450). Imaging was performed at the Athinoula A. Martinos Imaging Center at the McGovern Institute for Brain Research, Massachusetts Institute of Technology.

References

Abrams DA, Lynch CJ, Cheng KM, Phillips J, Supekar K, Ryali S, et al. 2013 Underconnectivity between voice-selective cortex and reward circuitry in children with autism. Proc Natl Acad Sci U S A 110:12060–12065.

Adolphs R. 2009. The social brain: neural basis of social knowledge. Annu Rev Psychol 60:693–716.

American Psychiatric Association. 1987. *Diagnostic and Statistical Manual of Mental Disorders*, 3rd ed., Rev. Washington, DC: American Psychiatric Association.

American Psychiatric Association. 1994. *Diagnostic and Statistical Manual of Mental Disorders*, 4th ed. Washington, DC: American Psychiatric Association.

American Psychiatric Association. 2013. *Diagnostic and Statistical Manual of Mental Disorders*, 5th ed. Arlington, VA: American Psychiatric Association.

Anderson JS, Druzgal TJ, Lopez-Larson M, Jeong EK, Desai K, Yurgelun-Todd D. 2011a. Network anticorrelations, global regression, and phase-shifted soft tissue correction. Hum Brain Mapp 32:919–934.

Anderson JS, Nielsen JA, Froehlich AL, DuBray MB, Druzgal TJ, Cariello AN, et al. 2011b. Functional connectivity magnetic resonance imaging classification of autism. Brain 134: 3742–3754.

Ashburner J, Friston KJ. 2005. Unified segmentation. Neuroimage 26:839–851.

Assaf M, Jagannathan K, Calhoun VD, Miller L, Stevens MC, Sahl R, et al. 2010. Abnormal functional connectivity of default mode sub-networks in autism spectrum disorder patients. Neuroimage 53:247–256.

Barttfeld P, Wicker B, Cukier S, Navarta S, Lew S, Leiguarda R, Sigman M. 2012. State-dependent changes of connectivity patterns and functional brain network topology in autism spectrum disorder. Neuropsychologia 50: 3653–3662.

Behzadi Y, Restom K, Liau J, Liu TT. 2007. A component based noise correction method (CompCor) for BOLD and perfusion based fMRI. Neuroimage 37:90–101.

Ben Shalom D, Mostofsky SH, Hazlett RL, Goldberg MC, Landa RJ, Faran Y, et al. 2006. Normal physiological emotions but differences in expression of conscious feelings in children with high-functioning autism. J Autism Dev Disord 36:395–400.

Berument SK, Rutter M, Lord C, Pickles A, Bailey A. 1999. Autism screening questionnaire: diagnostic validity. Br J Psychiatry 175:444–451.

Biswal B, Yetkin FZ, Haughton VM, Hyde JS. 1995. Functional connectivity in the motor cortex of resting human brain using echo-planar MRI. Magn Reson Med 34:537–541.

Blakemore SJ. 2008. The social brain in adolescence. Nat Rev Neurosci 9:267–277.

Blakemore SJ, Choudhury S. 2006. Development of the adolescent brain: implications for executive function and social cognition. J Child Psychol Psychiatry 47:296–312.

Blumberg SJ, Bramlett MD, Kogan MD, Schieve LA, Jones JR, Lu MC. 2013. Changes in prevalence of parent-reported autism spectrum disorder in school-aged U.S. children: 2007 to 2011–2012. Natl Health Stat Report 1–11.

Broyd SJ, Demanuele C, Debener S, Helps SK, James CJ, Sonuga-Barke EJ. 2009. Default-mode brain dysfunction in mental disorders: a systematic review. Neurosci Biobehav Rev 33:279–296.

Buckner RL, Andrews-Hanna JR, Schacter DL. 2008. The brain's default network: anatomy, function, and relevance to disease. Ann N Y Acad Sci 1124:1–38.

Calhoun VD, Adali T, Pearlson GD, Pekar JJ. 2001. A method for making group inferences from functional MRI data using independent component analysis. Hum Brain Mapp 14:140–151.

Caspers S, Geyer S, Schleicher A, Mohlberg H, Amunts K, Zilles K. 2006. The human inferior parietal cortex: cytoarchitectonic parcellation and interindividual variability. Neuroimage 33:430—448.

Castellanos FX, Margulies DS, Kelly C, Uddin LQ, Ghaffari M, Kirsch A, et al. 2008. Cingulate-precuneus interactions: a new locus of dysfunction in adult attention-deficit/hyperactivity disorder. Biol Psychiatry 63:332–337.

Chai XJ, Castanon AN, Ongur D, Whitfield-Gabrieli S. 2012. Anticorrelations in resting state networks without global signal regression. Neuroimage 59:1420–1428.

Chambers WJ, Puig-Antich J, Hirsch M, Paez P, Ambrosini PJ, Tabrizi MA, et al. 1985. The assessment of affective disorders in children and adolescents by semistructured interview. Test-retest reliability of the schedule for affective disorders and schizophrenia for school-age children, present episode version. Arch Gen Psychiatry 42:696–702.

Christoff K, Ream JM, Geddes LP, Gabrieli JD. 2003. Evaluating self-generated information: anterior prefrontal contributions to human cognition. Behav Neurosci 117:1161–1168.

Corbett BA, Carmean V, Ravizza S, Wendelken C, Henry ML, Carter C, Rivera SM. 2009. A functional and structural study of emotion and face processing in children with autism. Psychiatry Res 173:196–205.

Critchley HD, Daly EM, Bullmore ET, Williams SC, Van Amelsvoort T, Robertson DM, et al. 2000. The functional neuroanatomy of social behaviour: changes in cerebral blood flow when people with autistic disorder process facial expressions. Brain 123 (Pt 11):2203–2212.

D'argembeau A, Collette F, Van der Linden M, Laureys S, Del Fiore G, Degueldre C, Luxen A, Salmon E. 2005. Self-referential reflective activity and its relationship with rest: a PET study. Neuroimage 25:616–624.

Decety J, Lamm C. 2007. The role of the right temporoparietal junction in social interaction: how low-level computational processes contribute to meta-cognition. Neuroscientist 13: 580–593.

Di Martino A, Ross K, Uddin LQ, Sklar AB, Castellanos FX, Milham MP. 2009. Functional brain correlates of social and nonsocial processes in autism spectrum disorders: an activation likelihood estimation meta-analysis. Biol Psychiatry 65: 63–74.

Di Martino A, Zuo XN, Kelly C, Grzadzinski R, Mennes M, Schvarcz A, et al. 2013. Shared and distinct intrinsic functional network centrality in autism and attention-deficit/hyperactivity disorder. Biol Psychiatry 74:623–632.

Dosenbach NU, Nardos B, Cohen AL, Fair DA, Power JD, Church JA, et al. 2010. Prediction of individual brain maturity using fMRI. Science 329:1358–1361.

Doyle-Thomas KA, Lee W, Foster NE, Tryfon A, Ouimet T, Hyde KL, Evans AC, Lewis J, Zwaigenbaum L, Anagnostou E. 2015. Atypical functional brain connectivity during rest in autism spectrum disorders. Ann Neurol 77:866–876.

Drevets WC, Savitz J, Trimble M. 2008. The subgenual anterior cingulate cortex in mood disorders. CNS Spectr 13:663–681.

Ebisch SJ, Gallese V, Willems RM, Mantini D, Groen WB, Romani GL, et al. 2011. Altered intrinsic functional connectivity of anterior and posterior insula regions in high-functioning participants with autism spectrum disorder. Hum Brain Mapp 32:1013–1028.

Eilam-Stock T, Xu P, Cao M, Gu X, Van Dam NT, Anagnostou E, et al. 2014. Abnormal autonomic and associated brain activities during rest in autism spectrum disorder. Brain 137: 153–171.

First M, Gibbon M, Williams J, Spitzer R. 1996. *Structured Clinical Interview for DSM-IV Disorders: SCID SCREEN Patient Questionnaire Computer Program.* Washington, DC: American Psychiatric Press.

Fishman I, Keown CL, Lincoln AJ, Pineda JA, Muller RA. 2014. Atypical cross talk between mentalizing and mirror neuron networks in autism spectrum disorder. JAMA Psychiatry 71: 751–760.

Fox MD, Snyder AZ, Vincent JL, Corbetta M, Van Essen DC, Raichle ME. 2005. The human brain is intrinsically organized into dynamic, anticorrelated functional networks. Proc Natl Acad Sci U S A 102:9673–9678.

Fraley C, Raftery AE. 2012. mclust Version 4 for R: normal mixture modeling for model-based clustering, classification, and density estimation. Technical Report No. 597. Department of Statistics, University of Washington. https://www.stat.washington.edu/research/reports/2012/tr597.pdf Last accessed October 10, 2016.

Frith CD, Frith U. 2007. Social cognition in humans. Curr Biol 17:R724–R732.

Garrity AG, Pearlson GD, McKiernan K, Lloyd D, Kiehl KA, Calhoun VD. 2007. Aberrant ''default mode'' functional connectivity in schizophrenia. Am J Psychiatry 164:450–457.

Greicius MD, Flores BH, Menon V, Glover GH, Solvason HB, Kenna H, et al. 2007. Resting-state functional connectivity in major depression: abnormally increased contributions from subgenual cingulate cortex and thalamus. Biol Psychiatry 62:429–437.

Greicius MD, Krasnow B, Reiss AL, Menon V. 2003. Functional connectivity in the resting brain: a network analysis of the default mode hypothesis. Proc Natl Acad Sci U S A 100:253–258.

Hill E, Berthoz S, Frith U. 2004. Brief report: cognitive processing of own emotions in individuals with autistic spectrum disorder and in their relatives. J Autism Dev Disord 34:229–235.

Hollingshead AB. 1975. *Four Factor Index of Social Status*. New Haven, CT: Yale Press.

Igelstrom KM, Webb TW, Graziano MS. 2015. Neural processes in the human temporoparietal cortex separated by localized independent component analysis. J Neurosci 35:9432–9445.

Igelström KM, Webb TW, Graziano MS. 2016. Functional connectivity between the temporoparietal cortex and cerebellum in autism spectrum disorder. Cereb Cortex 27: 2617–2627.

Johnson SC, Baxter LC, Wilder LS, Pipe JG, Heiserman JE, Prigatano GP. 2002. Neural correlates of self-reflection. Brain 125:1808–1814.

Jolliffe IT. 2002. *Principal Component Analysis*. Springer Series in Statistics. New York, NY: Springer.

Kelley WM, Macrae CN, Wyland CL, Caglar S, Inati S, Heatherton TF. 2002. Finding the self? An event-related fMRI study. J Cogn Neurosci 14:785–794.

Kennedy DP, Courchesne E. 2008. Functional abnormalities of the default network during self- and other-reflection in autism. Soc Cogn Affect Neurosci 3:177–190.

Kleinhans NM, Richards T, Sterling L, Stegbauer KC, Mahurin R, Johnson LC, et al. 2008. Abnormal functional connectivity in autism spectrum disorders during face processing. Brain 131:1000–1012.

Koshino H, Kana RK, Keller TA, Cherkassky VL, Minshew NJ, Just MA. 2008. fMRI investigation of working memory for faces in autism: visual coding and underconnectivity with frontal areas. Cereb Cortex 18:289–300.

Kubit B, Jack AI. 2013. Rethinking the role of the rTPJ in attention and social cognition in light of the opposing domains hypothesis: findings from an ALE-based meta-analysis and resting-state functional connectivity. Front Hum Neurosci 7:323.

Lai MC, Lombardo MV, Chakrabarti B, Sadek SA, Pasco G, Wheelwright SJ, et al. 2010 A shift to randomness of brain oscillations in people with autism. Biol Psychiatry 68:1092–1099.

Liu H, Qin W, Li W, Fan L, Wang J, Jiang T, Yu C. 2013. Connectivity-based parcellation of the human frontal pole with diffusion tensor imaging. J Neurosci 33:6782–6790.

Lowe MJ, Dzemidzic M, Lurito JT, Mathews VP, Phillips MD. 2000. Correlations in low-frequency BOLD fluctuations reflect cortico-cortical connections. Neuroimage 12:582–587.

Lynch CJ, Uddin LQ, Supekar K, Khouzam A, Phillips J, Menon V. 2013. Default mode network in childhood autism: posteromedial cortex heterogeneity and relationship with social deficits. Biol Psychiatry 74:212–219.

Maldjian JA, Laurienti PJ, Kraft RA, Burdette JH. 2003. An automated method for neuroanatomic and cytoarchitectonic atlas-based interrogation of fMRI data sets. Neuroimage 19:1233–1239.

Meindl T, Teipel S, Elmouden R, Mueller S, Koch W, Dietrich O, et al. 2010. Test-retest reproducibility of the default-mode network in healthy individuals. Hum Brain Mapp 31:237–246.

Mitchell JP. 2009. Social psychology as a natural kind. Trends Cogn Sci 13:246–251.

Monk CS, Peltier SJ, Wiggins JL, Weng SJ, Carrasco M, Risi S, Lord C. 2009. Abnormalities of intrinsic functional connectivity in autism spectrum disorders. Neuroimage 47:764–772.

Moran JM, Macrae CN, Heatherton TF, Wyland CL, Kelley WM. 2006. Neuroanatomical evidence for distinct cognitive and affective components of self. J Cogn Neurosci 18:1586–1594.

Mueller S, Keeser D, Samson AC, Kirsch V, Blautzik J, Grothe M, et al. 2013. Convergent findings of altered functional and structural brain connectivity in individuals with high functioning autism: a multimodal MRI study. PLoS One 8:e67329.

Muller RA, Shih P, Keehn B, Deyoe JR, Leyden KM, Shukla DK. 2011. Underconnected, but how? A survey of functional connectivity MRI studies in autism spectrum disorders. Cereb Cortex 21:2233–2243.

Murphy K, Birn RM, Handwerker DA, Jones TB, Bandettini PA. 2009. The impact of global signal regression on resting state correlations: are anti-correlated networks introduced? Neuroimage 44:893–905.

Nicolson R, Szatmari P. 2003. Genetic and neurodevelopmental influences in autistic disorder. Can J Psychiatry 48:526–537.

Northoff G, Bermpohl F. Cortical midline structures and the self. 2004. Trends in cognitive sciences. Trends Cogn Sci 8:102–107.

Northoff G, Heinzel A, De Greck M, Bermpohl F, Dobrowolny H, Panksepp J. 2006. Self-referential processing in our brain—a meta-analysis of imaging studies on the self. Neuroimage 31:440–457.

Oldfield RC. 1971. The assessment and analysis of handedness: the Edinburgh inventory. Neuropsychologia 9:97–113.

Olson IR, Plotzker A, Ezzyat Y. 2007. The enigmatic temporal pole: a review of findings on social and emotional processing. Brain 130:1718–1731.

Orvaschel H. 1994. *Schedule for Affective Disorders and Schizophrenia for School-Age Children Epidemiologic Version*, 5th ed. Fort Lauderdale, FL: Nova Southeastern University, Center for Psychological Studies.

Orvaschel H, Puig-Antich J. 1987. *Schedule for Affective Disorders and Schizophrenia for School-Age Children: Epidemiologic Version*. Fort Lauderdale, FL: Nova University.

Pantelis PC, Byrge L, Tyszka JM, Adolphs R, Kennedy DP. 2015. A specific hypoactivation of right temporo-parietal junction/posterior superior temporal sulcus in response to socially awkward situations in autism. Soc Cogn Affect Neurosci 10:1348–1356.

Petrides M, Pandya DN. 2007. Efferent association pathways from the rostral prefrontal cortex in the macaque monkey. J Neurosci 27:11573–11586.

Pierce K, Muller RA, Ambrose J, Allen G, Courchesne E. 2001. Face processing occurs outside the fusiform 'face area' in autism: evidence from functional MRI. Brain 124:2059–2073.

Pierce K, Redcay E. 2008. Fusiform function in children with an autism spectrum disorder is a matter of ''who''. Biol Psychiatry 64:552–560.

R Core Team. 2015. R: A language and environment for statistical computing. R Foundation for Statistical Computing, Vienna, Austria. www.R-project.org Last accessed September 6, 2016.

Raichle ME. 2011. The restless brain. Brain Connect 1:3–12.

Raichle ME, Gusnard DA. 2005. Intrinsic brain activity sets the stage for expression of motivated behavior. J Comp Neurol 493:167–176.

Raichle ME, MacLeod AM, Snyder AZ, Powers WJ, Gusnard DA, Shulman GL. 2001. A default mode of brain function. Proc Natl Acad Sci U S A 98:676–682.

Ramnani N, Owen AM. 2004. Anterior prefrontal cortex: insights into function from anatomy and neuroimaging. Nat Rev Neurosci 5:184–194.

Redcay E, Moran JM, Mavros PL, Tager-Flusberg H, Gabrieli JD, Whitfield-Gabrieli S. 2013. Intrinsic functional network organization in high-functioning adolescents with autism spectrum disorder. Front Hum Neurosci 7:573.

Rieffe C, Meerum Terwogt M, Kotronopoulou K. 2007. Awareness of single and multiple emotions in high-functioning children with autism. J Autism Dev Disord 37:455–465.

Rudie JD, Shehzad Z, Hernandez LM, Colich NL, Bookheimer SY, Iacoboni M, Dapretto M. 2012. Reduced functional integration and segregation of distributed neural systems underlying social and emotional information processing in autism spectrum disorders. Cereb Cortex 22:1025–1037.

Rutter M, Bailey A, Lord C. 2003. *Social Communication Questionnaire*. Los Angeles, CA: Western Psychological Services.

Salmi J, Roine U, Glerean E, Lahnakoski J, Nieminen-von Wendt T, Tani P, et al. 2013. The brains of high functioning autistic individuals do not synchronize with those of others. Neuroimage Clin 3:489–497.

Scholz J, Triantafyllou C, Whitfield-Gabrieli S, Brown EN, Saxe R. 2009. Distinct regions of right temporo-parietal junction are selective for theory of mind and exogenous attention. PLoS One 4:e4869.

Schultz RT, Gauthier I, Klin A, Fulbright RK, Anderson AW, Volkmar F, et al. 2000. Abnormal ventral temporal cortical activity during face discrimination among individuals with autism and Asperger syndrome. Arch Gen Psychiatry 57: 331–340.

Seeley WW, Crawford RK, Zhou J, Miller BL, Greicius MD. 2009. Neurodegenerative diseases target large-scale human brain networks. Neuron 62:42–52.

Setsompop K, Gagoski BA, Polimeni JR, Witzel T, Wedeen VJ, Wald LL. 2012. Blipped-controlled aliasing in parallel imaging for simultaneous multislice echo planar imaging with reduced g-factor penalty. Magn Reson Med 67:1210–1224.

Sherman LE, Rudie JD, Pfeifer JH, Masten CL, McNealy K, Dapretto M. 2014. Development of the default mode and central executive networks across early adolescence: a longitudinal study. Dev Cogn Neurosci 10:148–159.

Stam CJ. 2014. Modern network science of neurological disorders. Nat Rev Neurosci 15:683–695.

Starck T, Nikkinen J, Rahko J, Remes J, Hurtig T, Haapsamo H, et al. 2013. Resting state fMRI reveals a default mode dissociation between retrosplenial and medial prefrontal subnetworks in ASD despite motion scrubbing. Front Hum Neurosci 7:802.

Tewarie P, van Dellen E, Hillebrand A, Stam CJ. 2015. The minimum spanning tree: an unbiased method for brain network analysis. Neuroimage 104:177–188.

Thesen S, Heid O, Mueller E, Schad LR. 2000 Prospective acquisition correction for head motion with image-based tracking for real-time fMRI. Magn Reson Med 44:457–465.

Uddin LQ. 2011. The self in autism: an emerging view from neuroimaging. Neurocase 17:201–208.

Uddin LQ, Supekar K, Amin H, Rykhlevskaia E, Nguyen DA, Greicius MD, Menon V. 2010. Dissociable connectivity within human angular gyrus and intraparietal sulcus: evidence from functional and structural connectivity. Cereb Cortex 20:2636–2646.

Uddin LQ, Supekar K, Menon V. 2013. Reconceptualizing functional brain connectivity in autism from a developmental perspective. Front Hum Neurosci 7:458.

von dem Hagen EA, Stoyanova RS, Baron-Cohen S, Calder AJ. 2013. Reduced functional connectivity within and between 'social' resting state networks in autism spectrum conditions. Soc Cogn Affect Neurosci 8:694–701.

Washington SD, Gordon EM, Brar J, Warburton S, Sawyer AT, Wolfe A, et al. 2014. Dysmaturation of the default mode network in autism. Hum Brain Mapp 35:1284–1296.

Wechsler D. 1999. *Wechsler Abbreviated Scale of Intelligence WASI: Manual*. San Antonio, TX: The Psychological Corporation.

Weng SJ, Wiggins JL, Peltier SJ, Carrasco M, Risi S, Lord C, Monk CS. 2010. Alterations of resting state functional connectivity in the default network in adolescents with autism spectrum disorders. Brain Res 1313:202–214.

Whitfield-Gabrieli S, Moran JM, Nieto-Castanon A, Triantafyllou C, Saxe R, Gabrieli JD. 2011. Associations and dissociations between default and self-reference networks in the human brain. Neuroimage 55:225–232.

Whitfield-Gabrieli S, Nieto-Castanon A. 2012. Conn: a functional connectivity toolbox for correlated and anticorrelated brain networks. Brain Connect 2:125–141.

Wiggins JL, Peltier SJ, Ashinoff S, Weng SJ, Carrasco M, Welsh RC, et al. 2011. Using a self-organizing map algorithm to detect age-related changes in functional connectivity during rest in autism spectrum disorders. Brain Res 1380:187–197.

You X, Norr M, Murphy E, Kuschner ES, Bal E, Gaillard WD, et al. 2013. Atypical modulation of distant functional connectivity by cognitive state in children with Autism Spectrum Disorders. Front Hum Neurosci 7:482.

Ypma RJ, Moseley RL, Holt RJ, Rughooputh N, Floris DL, Chura LR, Spencer MD, Baron-Cohen S, Suckling J, Bullmore ET, Rubinov M. 2016. Default mode hypoconnectivity underlies a sex-related autism spectrum. Biol Psychiatry Cogn Neurosci Neuroimaging 1:364–371.

Zhao F, Qiao L, Shi F, Yap PT, Shen D. 2016. Feature fusion via hierarchical supervised local CCA for diagnosis of autism spectrum disorder. Brain Imaging Behav [Epub ahead of print]; DOI: 10.1007/s11682-016-9587-5.

Address correspondence to:
Gagan Joshi
The Alan and Lorraine Bressler Clinical and Research Program for Autism Spectrum Disorder
Massachusetts General Hospital
55 Fruit Street, WRN 626
Boston, MA 02114

E-mail: Joshi.Gagan@MGH.Harvard.edu